NATIONAL ADVISORY COMMITTEE
FOR AERONAUTICS

TECHNICAL NOTE 3408

ONE-DIMENSIONAL CALCULATION OF FLOW IN A ROTATING

PASSAGE WITH EJECTION THROUGH A POROUS WALL

By E. R. G. Eckert, John N. B. Livingood, and Ernst I. Prasse

Lewis Flight Propulsion Laboratory
Cleveland, Ohio

Washington

March 1955

NATIONAL ADVISORY COMMITTEE FOR AERONAUTICS

TECHNICAL NOTE 3408

ONE-DIMENSIONAL CALCULATION OF FLOW IN A ROTATING PASSAGE

WITH EJECTION THROUGH A POROUS WALL

By E. R. G. Eckert, John N. B. Livingood, and Ernst I. Prasse

SUMMARY

In transpiration cooling of various structural elements in gas turbines, the coolant has to be ducted within passages to the porous walls through which it is ejected into the gas stream. The passages, often arranged in rotating parts, have to be designed in such a way as to ensure the proper local distribution of the coolant. In this report, a method is presented by which either the local permeability necessary for a prescribed distribution of the coolant flow or the coolant-flow distribution resulting from a prescribed local permeability can be predicted. The method is based on a one-dimensional treatment of the gas flow through a rotating channel with varying cross section and partially porous walls. The inlet pressure into the channel and the outside pressure along it are assumed prescribed. It is also stipulated that the passage ends blindly. However, the method can easily be extended to cover the situation where a certain mass flow leaves the open end of the passage.

The method was applied to a determination of conditions in rotating turbine blades with transpiration-cooled walls. The cooling air is assumed to flow from the blade root through several channels to the porous skin of the blades. For prescribed coolant-flow ejection rates necessary to maintain a constant porous wall temperature, considerable reduction in wall permeability from passage entrance to passage tip (blade root to blade tip) is required. In fact, such required variations will be extremely difficult to fabricate, and compromises between prescribed wall temperature and coolant-flow ejection may be necessary. For prescribed locally constant permeability, the mass-flow ejection rate increased from blade root to blade tip. The relative increase along the blade became smaller when the inlet pressure of the coolant at the blade root was increased. A large inlet pressure is therefore conducive to a uniform flow ejection rate and, accordingly, a more uniform blade wall temperature. In the investigated range, a passage area variation had practically no effect on flow ejection rates. For low Mach numbers at the passage inlet (below approximately 0.2 in the examples), the internal pressure distribution may well be approximated by consideration of rotational effects only. This leads to a considerable simplification in the calculation procedure.

INTRODUCTION

Transpiration cooling is considered as an effective means of keeping different structural elements in gas turbines at a temperature level sufficiently low for the material from which the elements are fabricated. Application of this cooling method is considered, for instance, for cooling the walls of combustion chambers and of rotating turbine blades. In both cases, passages have to be provided within which the coolant is ducted to the porous surfaces before it is finally ejected into the gas stream.

When transpiration cooling is applied to the rotating blades of the gas turbine, these passages will have to be arranged in the interior of the blade, for instance, as indicated in figure 1. The passages are closed at the top of the blade, and the cooling air leaves the passages through the porous blade surfaces. The flow of the cooling air through each of the passages is subject to friction forces along the passage wall, to centrifugal forces that tend to increase the pressure from the blade root towards the blade tip, and to pressure changes connected with the change in momentum of the cooling air on its way along the passage interior. The problem arises as to what local permeabilities along the passage are required to ensure a certain flow distribution or what the local flow distribution of the cooling air will be as it passes the porous surface with prescribed permeability and is ejected into the gas stream. In both cases, the calculation is complicated by the fact that the pressure outside the blade varies locally in radial direction as well as around the blade circumference.

A proper design of the blade requires the ability to predict the local flow rates through the porous blade walls. It is the purpose of this report to present a method by which the flow through passages with porous walls of the form indicated in figure 1 may be calculated. The method is based on a one-dimensional treatment of the flow and is essentially the same as presented in references 1 and 2. It is, however, especially adapted to the problem under investigation. The basic equations necessary for a solution of the problem are derived at first in a general way, so that they can be applied generally to calculate flow conditions in rotating passages. These equations are then adapted to the special conditions expected in gas turbine blades. The calculation procedure is discussed in detail, and the importance of the various parameters affecting the flow distribution is investigated in a number of numerical solutions.

SYMBOLS

The following symbols, with consistent units, are used:

A   cross-sectional (flow) area of passage

a   slope of dimensionless temperature ratio, $\tau = 1 + a\xi$

b	length of porous section of passage measured in circumferential direction
C_K	quantity containing permeability coefficient (see eq. (11))
$C_{K,dim}$	dimensionless quantity containing permeability coefficient (see eq. (17))
C_1	viscous-resistance coefficient
C_2	inertial-resistance coefficient
c_p	specific heat
D_h	hydraulic diameter of passage $\left(= \dfrac{4A}{circumference} \right)$
f	friction coefficient
f	function
K	permeability coefficient (see eq. (9))
L	length of passage
M	Mach number at passage inlet
m	mass coolant flow
N	$\omega L / \sqrt{\gamma R T_r}$
N″	$\omega L p_{i,r} / \left[R T_r \, (m/A)_r \right]$
n	exponent
p	pressure
R	gas constant
r	radius to element measured in plane of rotation (see fig. 1)
T	temperature of coolant
T_g	effective gas temperature
t	thickness of porous wall

V   flow velocity through porous wall (based on total porous surface area)

W   velocity of main flow through passage

x   distance from passage entrance (see fig. 1)

α dimensionless area ratio, A/A_r

β angle between velocity vector and direction of increasing radius

γ ratio of specific heats, 1.4

μ dimensionless coolant mass velocity ratio, $(m/A)/(m/A)_r$

ν kinematic viscosity

ξ dimensionless distance from passage entrance, x/L

π_e dimensionless external pressure ratio, $p_e/p_{i,r}$

π_i dimensionless internal pressure ratio, $p_i/p_{i,r}$

ρ density

τ dimensionless temperature ratio, T/T_r, except for τ_w (shearing stress at wall)

ω angular velocity

Subscripts:

e   external

i   internal

r   root (passage entrance)

s   considers rotating effects only

w   wall

0   NACA standard conditions

Superscript:

'   total condition

ANALYSIS

Derivation of Basic Equations

The basic equations used in this report are developed with the help of figure 1. This figure shows a portion of a channel, one wall of which is porous. The channel may rotate around the axis 1-1 with the angular velocity ω. Attention is fixed on a portion of fluid between the cross sections A and A + dA. This region is located at the distance r from the axis 1-1, and the axis of the channel is inclined under an angle β against the radial direction, where β is measured between the velocity vector and the direction of increasing r. The flow through the passage is assumed to be steady relative to the channel.

For steady-flow problems, application of Newton's second law of motion may be made by equating the net force acting on a control surface and the body forces acting on the fluid particles within the control area to the increase in momentum of the stream flowing through the stationary control surface. In the present case this law must be applied to a control area that is at rest relative to the channel. In figure 1 such a control area is indicated bounded by the two cross sections A and A + dA and by a surface located in immediate proximity to the inside wall of the channel between the two cross sections. Forces acting in flow direction on the control surface will be pressure forces in the two cross sections and along the channel wall, friction forces acting along the channel wall in the portion between the two cross sections, centrifugal forces, and Coriolis forces. The sum of all pressure forces is

$$p_1 A - (p_1 + dp_1)(A + dA) + \left(p_1 + \frac{dp_1}{2}\right) dA$$

if the pressure on the surface bounding the channel walls is approximated by $p_1 + dp_1/2$. Neglecting second-order terms reduces the pressure forces to

$$- A\, dp_1$$

When the friction factor f is defined by the equation

$$\tau_w = \frac{f \rho W^2}{8}$$

(τ_w denoting the shearing stress at the wall), the friction force can be expressed in the following way:

$$-f \frac{dx}{D_h} \rho \frac{W^2}{2} A$$

Body forces, caused by centrifugal acceleration of the fluid particles, can be written as

$$\rho A r \omega^2 \cos \beta \, dx$$

The Coriolis force is oriented normal to the flow direction through the passage and has no component in the direction of the passage axis. The increase in momentum of the stream flowing through the control surfaces is

$$(m + dm)(W + dW) - mW$$

or

$$m \, dW + W \, dm.$$

Equating the various force terms with the change in momentum results in

$$- A \, dp_i - \frac{f}{2} \frac{\rho W^2 A}{D_h} dx + \rho A r \omega^2 \cos \beta \, dx = m \, dW + W \, dm \qquad (1)$$

Use of the continuity equation

$$m = \rho A W \qquad (2)$$

the equation of state

$$p_i = \rho R T \qquad (3)$$

and the relation

$$\frac{dm}{dx} = A \frac{d\left(\frac{m}{A}\right)}{dx} + \frac{m}{A} \frac{dA}{dx} \qquad (4)$$

in equation (1) leads to

$$\left[1 - \left(\frac{m}{A}\right)^2 \frac{RT}{p_i^2} \right] \frac{dp_i}{dx} = \frac{p_i}{RT} r \omega^2 \cos \beta - \frac{2RT}{p_i} \left(\frac{m}{A}\right) \frac{d\left(\frac{m}{A}\right)}{dx} -$$

$$\left(\frac{m}{A}\right)^2 \left(\frac{R}{p_i}\right) \left(\frac{dT}{dx} + \frac{T}{A} \frac{dA}{dx} + \frac{fT}{2D_h}\right) \qquad (5)$$

3529

The static temperature T is determined by the rate at which internal energy in the flowing gas stream is converted into kinetic energy, as well as by the rate with which heat is added to or subtracted from the gas stream. For high-velocity flow in which the conversion of internal energy into kinetic energy becomes an important factor, it would be more appropriate to calculate with the total temperature, which is directly connected with the rate of heat addition, than with the static temperature. This conversion can be made with the help of the following equation:

$$T' = T + \frac{W^2}{2c_p} = T + \frac{\left(\frac{m}{A}\right)^2 R^2 T^2}{2p_i^2 c_p}$$

The change from the static to the total temperature, however, complicates equation (5) considerably. On the one hand, the flow velocities in the passages are usually small enough to make the temperature change connected with the conversion of internal into kinetic energy small. On the other hand, the rate of heat addition to the coolant on its way through the flow channel usually is not too well known and has to be estimated. For these reasons, the static temperature is maintained in the following calculations. It is assumed that the variation of the static temperature along the coolant flow channel is known.

In equation (5), the specific mass flow m/A, the internal pressure p_i, the radius r, the tangential velocity $r\omega$, and the cross-sectional area A are generally functions of the distance x from the channel entrance measured along the channel axis. The temperature T may also vary along x.

A second expression including the same variables as functions of the distance from the passage entrance can be obtained from a consideration of the pressure drop through the porous wall when the pressure distribution along the outside of the passage is prescribed. The mass velocity of the coolant ejected through the porous wall at any location multiplied by the width of the porous portion of the channel wall measured in circumferential direction equals the rate of change of the coolant mass flow passing through the passage at that location; that is,

$$-b(\rho V) = \frac{dm}{dx} \tag{6}$$

The quantity ρV is the average mass-flow rate over the channel width b. The negative sign appears in the left member of equation (6) when the velocity is considered positive for flow leaving the channel through the porous wall. Reference 3 shows that the mass velocity of a gas flowing through a porous wall is connected with the difference in the squares of the pressures acting on both sides of the wall, through the equation

$$\frac{p_1^2 - p_e^2}{t} = C_1(2RT\rho\nu)(\rho V) + C_2\ 2RT(\rho V)^2 \tag{7}$$

Values of C_1 and C_2 must be determined experimentally for each porous material.

Equation (7) may be referred to measurements at standard conditions by transformation into (see ref. 4)

$$\frac{p_1^2 - p_e^2}{t}\left(\frac{\rho_0\nu_0}{\rho\nu}\right)^2 \frac{T_0}{T} = f\left(\rho V\ \frac{\rho_0\nu_0}{\rho\nu}\right) \tag{8}$$

The parameters appearing on both sides of equation (8), when plotted on log-log coordinates for several types of porous materials, indicate an almost linear variation over a fairly wide range of flow for any of the materials. As a consequence, equation (8) may be well approximated by

$$\rho V\ \frac{\rho_0\nu_0}{\rho\nu} = \left[\frac{K}{t}\left(\frac{\rho_0\nu_0}{\rho\nu}\right)^2 \frac{T_0}{T}\left(p_1^2 - p_e^2\right)\right]^n \tag{9}$$

where K is the permeability of the material. On a log-log plot of $\dfrac{p_1^2 - p_e^2}{t}\left(\dfrac{\rho_0\nu_0}{\rho\nu}\right)^2 \dfrac{T_0}{T}$ against $\rho V(\rho_0\nu_0/\rho\nu)$, the intercept of the curve for a given porous material on the log $\rho V(\rho_0\nu_0/\rho\nu)$ axis is the value of n log K for that material. This definition of K is similar, but not identical, to that normally used. For the purpose of this calculation, equation (9) is simplified to

$$\rho V = C_K\left(p_1^2 - p_e^2\right)^n \tag{10}$$

by introduction of the parameter

$$C_K = \left(\frac{K}{t}\right)^n \left(\frac{\rho_0\nu_0}{\rho\nu}\right)^{2n-1} \left(\frac{T_0}{T}\right)^n \tag{11}$$

The values of C_K and n are functions of the porous material; they also vary slightly with the specific mass flow $\rho V(\rho_0\nu_0/\rho\nu)$. The value of C_K is a function of the material permeability and thickness, and of cooling-air properties based on porous-wall temperature. Substitution of equations (4) and (10) into equation (6) gives the desired relation:

$$A \frac{d\left(\frac{m}{A}\right)}{dx} + \frac{m}{A} \frac{dA}{dx} = -bC_K \left(p_i^2 - p_e^2\right)^n \tag{12}$$

Equations (5) and (12) are two equations from which two unknown values can be calculated.

Reduction to Dimensionless Form

In order to make the results of calculations more generally applicable, it is advantageous to change equations (5) and (12) to dimensionless form. For this purpose, the following substitutions are made (the dimensionless variables are denoted by Greek letters corresponding to the English letters for the dimensioned quantities, and the constants by English capital letters):

$$
\left.
\begin{aligned}
\mu &= \frac{m}{A} \Big/ \left(\frac{m}{A}\right)_r \\[2mm]
\xi &= \frac{x}{L} \\[2mm]
\pi_i &= \frac{p_i}{p_{i,r}} \\[2mm]
\pi_e &= \frac{p_e}{p_{i,r}} \\[2mm]
\tau &= \frac{T}{T_r} \\[2mm]
\alpha &= \frac{A}{A_r} \\[2mm]
M &= \frac{\left(\frac{m}{A}\right)_r}{p_{i,r}} \sqrt{\frac{RT_r}{\gamma}} \\[2mm]
N'' &= \frac{\omega L p_{i,r}}{R T_r \left(\frac{m}{A}\right)_r} \\[2mm]
N &= N'' M = \frac{\omega L}{\sqrt{\gamma R T_r}}
\end{aligned}
\right\} \tag{13}
$$

It can be shown easily that the parameter M is the Mach number of the flow at the passage inlet. The parameter N'' is essentially the square root of the ratio of the centrifugal force to an inertia force. This can be seen from the following transformation:

$$N''^2 = \frac{\omega^2 L^2 p_{i,r}^2}{R^2 T_r^2 \left(\frac{m}{A}\right)_r^2} = \frac{\rho_r^2 \omega^2 L^2}{\rho_r^2 W_r^2} = \frac{L}{2r_r} \frac{\rho_r r_r \omega^2}{\rho_r \left(\frac{W_r^2}{2L}\right)}$$

The right-hand term is, in addition to the length ratio $L/2r_r$, the ratio of the centrifugal force per unit fluid volume at the passage entrance to the inertia force that would be necessary to slow down the fluid particle from an initial velocity W_r to the velocity zero over a length equal to the channel length L.

Use of these substitutions in equations (5), (10), and (12) gives the following dimensionless equations:

$$\left(1 - \frac{\gamma M^2 \mu^2 \tau}{\pi_i^2}\right) \frac{d\pi_i}{d\xi} = \frac{r}{L} \frac{\gamma \pi_i N^2}{\tau} (\cos \beta) - \frac{2\gamma M^2 \mu \tau}{\pi_i} \frac{d\mu}{d\xi} - \frac{\gamma M^2 \mu^2}{\pi_i} \left(\frac{f}{2} \frac{L}{D_h} \tau + \frac{d\tau}{d\xi} + \frac{\tau}{\alpha} \frac{d\alpha}{d\xi}\right)$$

$$(14)$$

$$\frac{\rho V}{\left(\frac{m}{A}\right)_r} = C_{K,dim}\left(\pi_i^2 - \pi_e^2\right)^n \qquad (15)$$

$$\frac{d\mu}{d\xi} = -\frac{\mu}{\alpha} \frac{d\alpha}{d\xi} - \frac{1}{\alpha} \frac{bL}{A_r} C_{K,dim}\left(\pi_i^2 - \pi_e^2\right)^n \qquad (16)$$

where

$$C_{K,dim} = \left[\frac{\left(p_{i,r}^2\right)^n}{\left(\frac{m}{A}\right)_r}\right] C_K \qquad (17)$$

CALCULATION PROCEDURE

The two equations (5) and (12) or (14) and (16) can be used to calculate two of the parameters that depend on x if the rest of the

parameters and an appropriate set of boundary conditions are prescribed. Two problems are most frequently encountered in applying this analysis to design calculations: (1) A passage of prescribed geometry is closed at one end and fed at the other end by gas of a prescribed state. The pressure along the outside of the porous passage wall of prescribed material (C_K and n known) and the local distribution of the flow ejection through the porous wall are prescribed as well. The local distribution of the permeability of the channel wall has to be determined in such a way that the required flow rate through this wall (for instance, to obtain a desired wall temperature distribution) is obtained. (2) The passage geometry as well as the permeability of the porous portion of the channel walls of known material is prescribed. The channel is again closed at one end and fed at the other end with gas of a prescribed state. The outside pressure distribution is known. The distribution of the local flow rate through the porous wall has to be determined.

The first problem is the easier one to calculate, because, with the local flow rate prescribed, the mass flow within the channel may be obtained from integration of equation (6). Equation (5) or (14) then can be used to calculate the internal pressure distribution along the passage, because all the other terms in either equation are known, and equation (10) (or (15)) can then be solved for the constants C_K or $C_{K,dim}$, which determine the required local permeability of the porous wall.

Case (2) makes it necessary to solve equations (5) and (12) or (14) and (16) simultaneously for the two unknowns p_i or π_i and m/A or μ, the internal pressure and the mass velocity, respectively.

A simplification of the outlined calculation procedure, investigated for assumed radial passages, considers only centrifugal and pressure forces in the balance of forces acting on the control area. Equation (1) reduces to

$$- A\, dp_{i,s} + \rho A r \omega^2\, dx = 0$$

and equation (14) reduces to

$$\frac{d\pi_{i,s}}{d\xi} = \left(\frac{r_r}{L} + \xi\right) \frac{\gamma \pi_{i,s} N^2}{\tau} \tag{18}$$

The numerical examples presented later in this report are obtained for an assumed linear variation in cooling-air temperature; as a consequence, τ also varies linearly in the form

$$\tau = 1 + a\xi$$

With this expression for τ inserted in equation (18), direct integration results in

$$\ln \pi_{i,s} = \frac{\gamma N^2}{a^2} \left(\frac{r_r}{L} a - 1 \right) \ln (1 + a\xi) + \frac{\gamma N^2}{a} \xi \qquad (19)$$

The dimensionless pressure $\pi_{i,s}$ in the passage is now independent of the coolant flow. The conditions under which the simplified procedure can be used are discussed later.

NUMERICAL EXAMPLES

Sample calculations for each of the two problems previously discussed were made for cooling-air passages I and II of the turbine blade shown in figure 2. The parameters needed in the calculations are indicated in the figure legend. They were chosen to correspond to conditions prevailing in a test engine available at the NACA Lewis laboratory for the testing of turbine blades. Passages I and II were assumed to be radial passages ($\beta = 0$). The cross-sectional area of passage II is assumed to decrease linearly along the blade span to a value at the tip which is half that at the root. That of passage I is constant for all calculations except one, the case where the effect of area variation on flow conditions was investigated. For this case, two arbitrary passage area variations to be discussed later were considered, in addition to the case of constant area. Poroloy wire cloth was selected as the porous material for the turbine blade skin, constituting the porous side of each passage. An empirical equation supplied by the manufacturers of Poroloy (ref. 5) and valid for flow rates between 0.0001 and 0.1 pound per second per square inch gives the value n in equation (10) as $5/8$. The expression

$$C_K = \left(\frac{K}{t} \right)^n \left(\frac{\rho_0 \nu_0}{\rho \nu} \right)^{2n-1} \left(\frac{T_0}{T} \right)^n$$

will be used later to determine the permeability per unit thickness K/t of the porous side of passages I and II (see fig. 2).

The external pressure variations along passages I and II are also shown in figure 2. These spanwise pressure distributions were obtained from calculated velocity and pressure distributions around the blade periphery at three spanwise locations. The effective gas temperature profile along the blade span shown in figure 2 was determined experimentally with uncooled blades of the same geometry in a test engine. The inlet cooling-air temperature was assumed as $T_r = 640^\circ$ R. A linear increase of approximately 200° F in cooling-air temperature through the

blade span was assumed arbitrarily. The friction factor f indicated
in figure 2 was obtained from the relation valid for turbulent flow
through a tube. It corresponds to a Reynolds number of about 2000 when
this parameter is based on the hydraulic diameter of the passage. Ac-
tually, the Reynolds number, and therefore the friction factor, varies
along the passage. This variation was neglected in the present
calculations.

The following dimensionless quantities were obtained from the pa-
rameters in figure 2; they are held fixed throughout the calculations:

$$f = 0.0475$$

$$\tau = 1 + 0.328\ \xi$$

$$r_r/L = 2.569$$

$$N = 0.2916$$

Permeability Requirements for Prescribed Flow Ejection

The determination of the permeability of the porous wall necessary
to fulfill prescribed flow ejection distributions for the two passages·
of the blade shown in figure 2 will be considered first. The results
of these calculations are presented in figures 3 to 6. The two passages
were chosen so that laminar boundary-layer flow is expected along the
outside blade surface adjacent to one passage (I) and turbulent flow
along the outside blade surface adjacent to the other passage (II) when
transition is estimated from the pressure distribution around the blade
periphery. A blade wall temperature of $600°$ F was prescribed. The
spanwise cooling-air-flow rate ρV can be calculated from the data pre-
sented and from the condition that the blade temperature is constant over
the surface (ref. 4). The cooling-air-flow distribution and a knowledge
of b, the circumferential length of the porous section of the passage
at each spanwise position, permit the integration of equation (6) and
hence the determination of the distribution of the mass flow m through-
out the passage. After conversion to the dimensionless mass-flow pa-
rameter μ, equation (14) can be solved for the dimensionless internal
pressure distribution π_i. For the integration of equation (14), the
cooling-air pressure at the entrance of the passage must be known. For
this calculation, the value of the dimensionless external pressure at
the root $\pi_{e,r}$ was assumed to be 0.95. From the internal and external
dimensionless pressure ratios π_i and π_e, respectively, the dimension-
less permeability parameter $C_{K,dim}$ is obtained from equation (15).
This parameter is valid for any porous material for which the mass flow

is described by equation (12). For Poroloy the desired permeability per unit thickness is determined from the expression

$$\frac{K}{t} = \left[\left(\frac{m}{A}\right)_r c_{K,dim}\right]^{\frac{1}{n}} \left(\frac{\rho v}{\rho_0 v_0}\right)^{2-\frac{1}{n}} \frac{1}{p_{i,r}^2} \frac{T}{T_0}$$

resulting from use of equations (17) and (11).

Figure 3 shows, in dimensionless form, the results of this calculation, namely, the internal mass-flow distribution μ (which is nearly linear) and the internal pressure distribution π_i as functions of the dimensionless distance $\xi = x/L$ for passage I, whose porous wall is exposed to laminar external flow. The prescribed external pressure distribution π_e is also shown once more for comparison. Figure 4 shows the dimensionless permeability parameter $c_{K,dim}$, which is valid for any porous material for which equation (10) holds, and the permeability distribution K/t required to satisfy the prescribed cooling-air ejection rates through the porous Poroloy wall. A rapid reduction in blade permeability or a corresponding increase in wall thickness is required near the lower quarter-span of the passage, a more gradual permeability reduction or thickness increase to about the three-quarter-span location, and a nearly constant permeability or thickness in the region near the blade tip. Such a permeability or thickness variation will be extremely difficult to fabricate; and, in all probability, some sort of compromise between prescribed wall temperature (and corresponding prescribed coolant-flow ejection ρV) and a more readily obtainable permeability or thickness variation will be necessary.

A variation of the parameter K/t as shown in figure 4 is also often unfavorable with regard to stress, because it may mean heavier material for the blade shell near the tip of the blade. It is easily understandable that the variation of the parameter K/t along the blade length becomes smaller when the pressure at the passage inlet is increased. This is shown in more detail in some later figures. The result of the simplified calculation procedure (eq. (19)) is shown in figure 3 as the dashed line $\pi_{i,s}$. It can be observed that the difference between the result of the original calculation (the solid line π_i) and the result of the simplified procedure (the dashed line $\pi_{i,s}$) is very small under the assumed parameters.

Passage II differs from passage I by the fact that the gas flow around the blade is expected to produce a turbulent boundary layer adjacent to passage II. Consequently, the coolant-flow ejection ρV

required to maintain a blade wall temperature of 600° F is considerably larger than for passage I. This distribution along the span of passage II was calculated by the method discussed in reference 4 and is shown in in figure 5. The cross-sectional area of passage II was assumed to decrease linearly from blade root to tip; its value at the tip was half its value at the root. In algebraic form, the dimensionless area of passage II may be expressed as $\alpha = 1 - 0.5\xi$. The calculation proceeded as in the previously described case. The results are plotted in figures 5 and 6. Dimensionless distributions of external pressure π_e, internal pressure π_i, and mass velocity μ are shown as functions of the dimensionless distance $\xi = x/L$ in figure 5. The variation of the cross-sectional area of the passage is reflected in the distribution of mass velocity m/A. The dimensionless permeability parameter $C_{K,dim}$ and the distribution of K/t are presented in figure 6. The variation of these parameters over the blade height is qualitatively the same as for passage I. The required permeabilities, however, are considerably larger for passage II in order to accommodate the larger coolant-flow rates.

The dimensionless internal pressure distribution $\pi_{i,s}$ calculated by the simplified equation is inserted in figure 5 as the dashed line. The difference between the solid line pressure distribution π_i obtained by use of equation (14) and the dashed line in figure 5 is larger than it was for passage I (fig. 3). Since the calculation is considerably simplified by use of equation (18) instead of equation (14), it is important to know when this simplification is permissible. This will be discussed in detail later.

Flow Ejection Distribution for Prescribed Permeability

The determination of the flow ejection distribution for a prescribed porous-wall permeability requires the simultaneous solution of equations (14) and (16). The two boundary conditions that must be fulfilled apply at opposite ends of the passage; that is, the dimensionless internal pressure at the passage entrance $\pi_{i,r}$ must equal unity, and the dimensionless mass velocity μ must reduce to zero at the passage tip. Moreover, π_i must exceed (or in the limiting case, equal) the dimensionless external pressure π_e everywhere along the passage to ensure flow through the wall in the proper direction. For a prescribed distribution of the outside pressure π_e, a unique μ distribution that reduces to zero at the passage tip can be found. However, this distribution can only be found by a trial-and-error procedure. It is necessary to assume values of $p_{i,r}$ and $(m/A)_r$ at the passage entrance, to solve the equations numerically, and to check the value of μ at the passage tip. In general, several trials will be required before the value $\mu = 0$ at the tip is obtained.

Calculations were made for the determination of the flow ejection distributions in passage I for three assumed values of the internal pressure at the passage entrance $p_{i,r}$ (and hence for three distributions of $\pi_e = p_e/p_{i,r}$) for a passage with a porous wall whose permeability is $C_K = 10^{-5}$ $ft^{1/2}/(sec)(lb^{1/4})$. Uniform porous-wall thickness and constant passage area ($\alpha = 1$) were assumed. The external pressure distributions π_e, the internal pressure distributions π_i, and the internal flow distributions μ are shown in figure 7. Also shown, as a dashed curve, is the internal pressure distribution $\pi_{i,s}$, which includes rotational effects only and was calculated by use of equation (19). Only slight variations in the internal pressure distribution π_i result from variation of the pressure with which the cooling air enters the blade root. Moreover, the internal pressure distribution $\pi_{i,s}$ obtained by use of equation (18) is only slightly different from the other π_i distributions obtained by use of equation (14). For this blade passage, therefore, the simplified procedure would give practically the same results as the more complicated solution involving equation (14). The saving in time is especially large in this case, since no trial-and-error procedure has to be employed when equation (18) is used.

The distribution of the air ejection rate ρV is shown in figure 8. As expected, the ρV values increase as $\pi_{e,r}$ decreases. Also, the ratio of the ρV value at any location to the value at the passage entrance changes less along the blade length with increasing inlet pressure. The ρV distribution that results in a constant blade shell temperature is nearly constant spanwise, as can be seen from figure 3. A constant value of K/t for the porous wall will therefore lead to a blade temperature that decreases from root to tip. To make this decrease small, the cooling-air inlet pressure at the blade root should be made as large as possible.

Figure 8 can be used to estimate how much more cooling air is required for passage I when the porous wall has constant permeability than when the permeability varies spanwise so as to give the constant or nearly constant coolant-flow rate ρV necessary to maintain a constant spanwise wall temperature. For purpose of comparison, it may be assumed that the wall permeability and inlet pressure at the passage entrance are adjusted so that the coolant flow ρV (and hence also the wall temperature) at the base is the same for both cases. It is then seen that, for the cases of a constant wall permeability with $\pi_{e,r} = 0.8$ and 0.6, the corresponding excess use of cooling air over the ideal case of a constant spanwise ρV is approximately 77 percent and 45 percent, respectively. For the limiting case where $\pi_{e,r} = 1.0$, the coolant flow ρV is zero at the blade root, and the condition of a constant spanwise coolant flow ρV reduces to the case of an impermeable blade wall.

A series of calculations was made for the same passage, the same wall permeability, the same external pressure distribution corresponding to $\pi_{e,r} = 0.8$, but for passages whose flow areas increase $(\alpha = 1 + 0.5\,\xi)$, are constant $(\alpha = 1)$, and decrease $(\alpha = 1 - 0.5\,\xi)$ in flow direction, respectively. Figures 9 and 10 present the results of these calculations. Figure 9 shows very little variation in the various π_i distributions (including $\pi_{i,s}$), in spite of rather marked variations in the mass velocity distributions μ. Accordingly, the ρV distributions indicate (fig. 10) that passage flow-area variation has an almost negligible influence on the flow ejection rates.

From the fact that the π_i curves in figure 9 are all in reasonably close agreement with the $\pi_{i,s}$ curve resulting from the simplified calculation (eq. (19)), it may be deduced that changes in the variation of cross-sectional area do not cause appreciable differences between the pressure distributions obtained by the two calculation procedures. It can be concluded, therefore, that the rate of coolant flow, or Mach number, is the determining parameter in this regard.

Examination of equations (14) and (18) reveals that the two solutions are identical for the case of zero coolant flow $(M = 0)$; and, hence, for small Mach numbers M good agreement between the solutions for π_i and $\pi_{i,s}$ (eqs. (14) and (18), respectively) is expected. That this is the case for the present calculations can be seen from figures 3, 5, 7, and 9. In figure 3, the Mach number is very small $(M = 0.059)$, and the solutions for π_i and $\pi_{i,s}$ are practically identical. In figure 7, the solutions for π_i are for Mach numbers M of 0.135, 0.185, and 0.228; the corresponding maximum percentage differences between π_i and $\pi_{i,s}$ are $\dfrac{\pi_i - \pi_{i,s}}{\pi_{i,s}} \times 100\% = 0.9$, 1.8, and 3.1 percent, respectively. In figure 9, where all solutions are for an essentially constant Mach number of 0.185, the maximum percentage difference between π_i and $\pi_{i,s}$ is only 2.1 percent. The solution for π_i presented in figure 5, however, represents a comparatively high coolant-flow rate with a Mach number of 0.350, and the maximum percentage difference between π_i and $\pi_{i,s}$ is 8.6 percent, an appreciable amount. From these results, it appears that the use of the simplified solution for the internal pressure $\pi_{i,s}$ given by equation (19) results in an error of order not more than approximately 2 percent from the exact solution, as long as the coolant-flow Mach number does not greatly exceed 0.2.

SUMMARY OF RESULTS

A one-dimensional method that permits the calculation of local permeability for prescribed coolant flow (or the solution of the inverse problem) for a rotating passage with varying cross section and partially porous walls was developed. A knowledge of the temperature distribution of the cooling air inside the passage, the outside pressure along the passage, and the passage geometry is required. Solutions to the first problem were obtained by solving independently a pair of first-order differential equations. For the inverse problem, a simultaneous solution of a pair of equations is required; a trial-and-error procedure has to be applied in this case.

Solutions to both problems were obtained for several blind radial passages in a transpiration-cooled turbine rotor blade. The results of this investigation are as follows:

1. For prescribed coolant-flow ejection rates necessary to maintain a constant porous-wall temperature for both a constant-area passage exposed to external laminar-flow conditions and a variable-area passage exposed to external turbulent-flow conditions, considerable reduction in permeability or increase in thickness is required from blade root to blade tip. In either case, a rapid reduction in permeability or increase in thickness is required near the root of the blade; the reduction tends to level off considerably beyond this point.

2. Permeability or thickness variations like those necessary to maintain a constant wall temperature throughout appear extremely difficult to obtain with present-day materials, and some compromises between prescribed wall temperature and a more readily obtainable permeability or thickness distribution will undoubtedly be necessary. These variations will probably require some increase in shell thickness near the tip of the blade and, as a consequence, they might be unfavorable from stress considerations.

3. For prescribed locally constant permeability, the mass-flow ejection rate increases from blade root to blade tip. As the passage inlet pressure is increased, the relative increase in flow ejection rate along the blade height becomes less. Consequently, a large inlet pressure will result in a more nearly uniform flow ejection rate.

4. For prescribed locally constant permeability, variations in passage cross-sectional area had practically no influence on flow ejection rates.

5. The internal pressure distribution of cooling air in a rotating passage can be approximated by balancing the centrifugal force due to rotation with the pressure forces only. This approximation can be

applied to the solution of both types of problems discussed above. For many cases of practical importance, the simplified differential equation can be integrated directly to obtain the pressure distribution, thus eliminating the numerical process necessary for the complete solution. The complete solution and the approximate solution converge for zero coolant flow. The results presented in this report indicate that the complete solution for the internal pressure is well approximated by the simplified solution, for cooling-air Mach numbers at the passage entrance that do not greatly exceed 0.2. The maximum difference between the complete and approximate solutions is then of the order of 2 percent.

Lewis Flight Propulsion Laboratory
        National Advisory Committee for Aeronautics
                Cleveland, Ohio, November 18, 1954

REFERENCES

1. Shapiro, Ascher H.: The Dynamics and Thermodynamics of Compressible Fluid Flow. Ronald Press Co. (N. Y.), 1953.

2. Brown, W. Byron, and Rossbach, Richard J.: Numerical Solution of Equations for One-Dimensional Gas Flow in Rotating Coolant Passages. NACA RM E50E04, 1950.

3. Green, Leon, Jr.: Fluid Flow Through Porous Metals. Prog. Rep. No. 4-111, Jet Prop. Lab., C.I.T., Aug. 19, 1949. (Ord. Dept. Contract No. W-04-200-ORD-455.)

4. Livingood, J. N. B., and Eckert, E. R. G.: Calculation of Transpiration-Cooled Gas-Turbine Blades. Trans. A.S.M.E., vol. 75, no. 7, Oct. 1953, pp. 1271-1278.

5. Anon.: Introducing a New Porous Metal - Poroloy. Poroloy Equipment, Inc., Pacoima (Calif.).
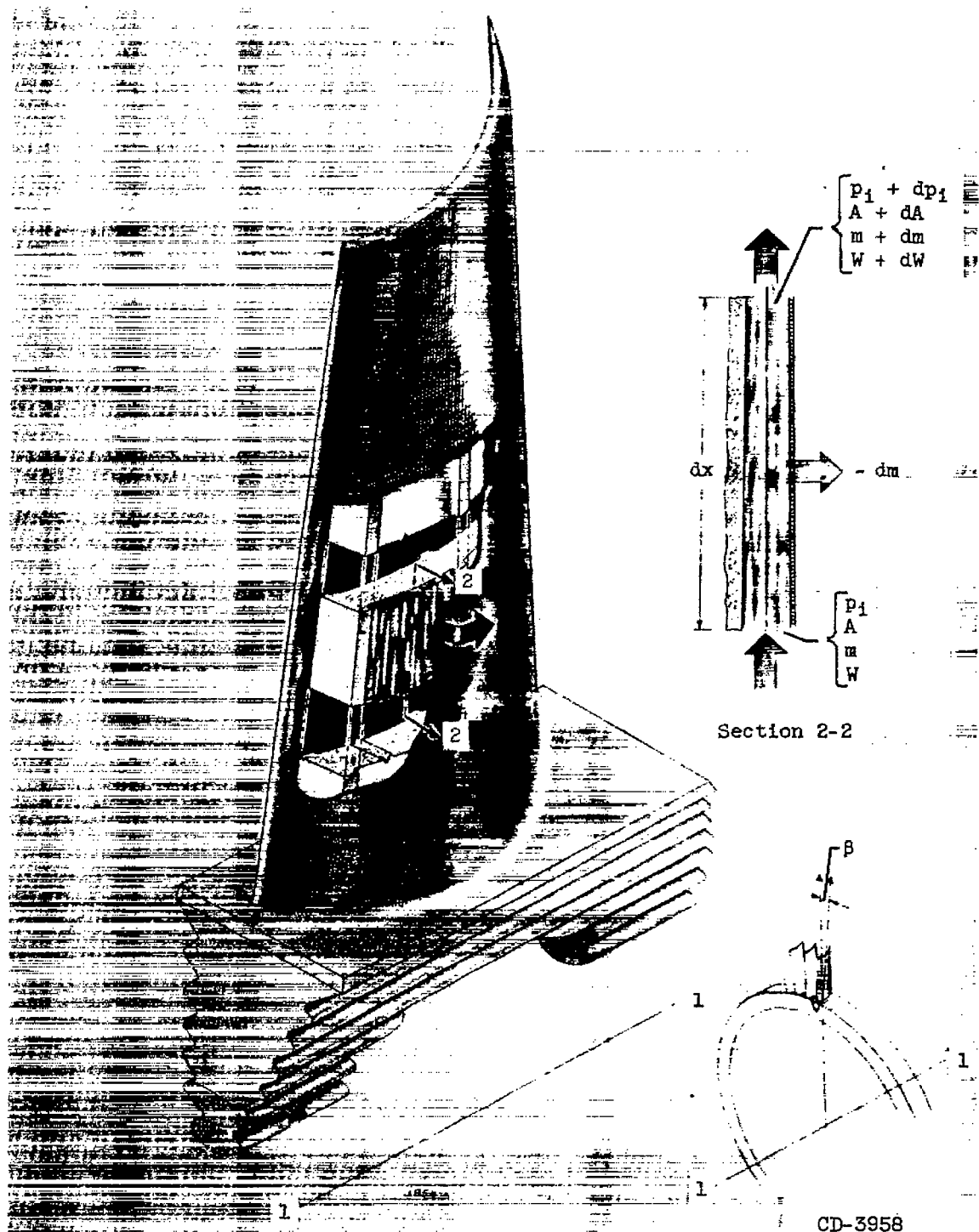
Figure 1. - Transpiration-cooled turbine blade and detailed element of
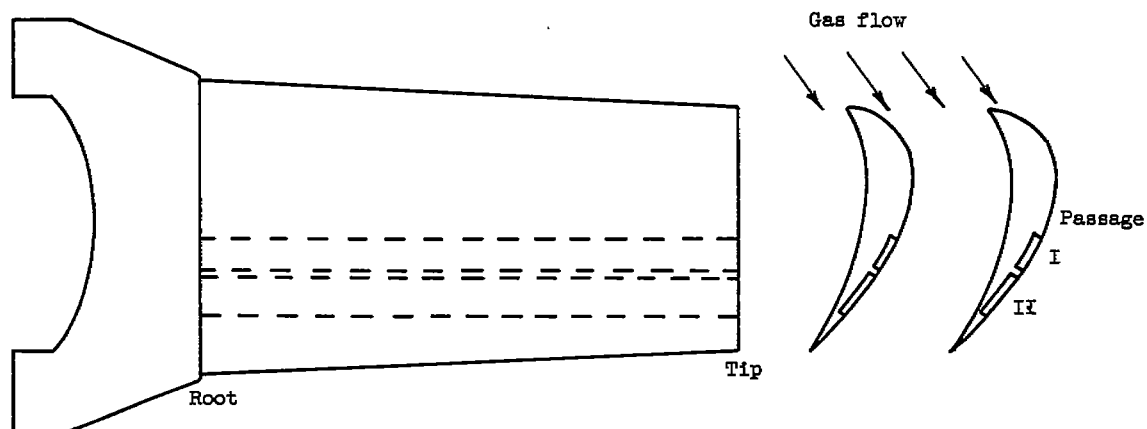control area used in derivation of basic equations.
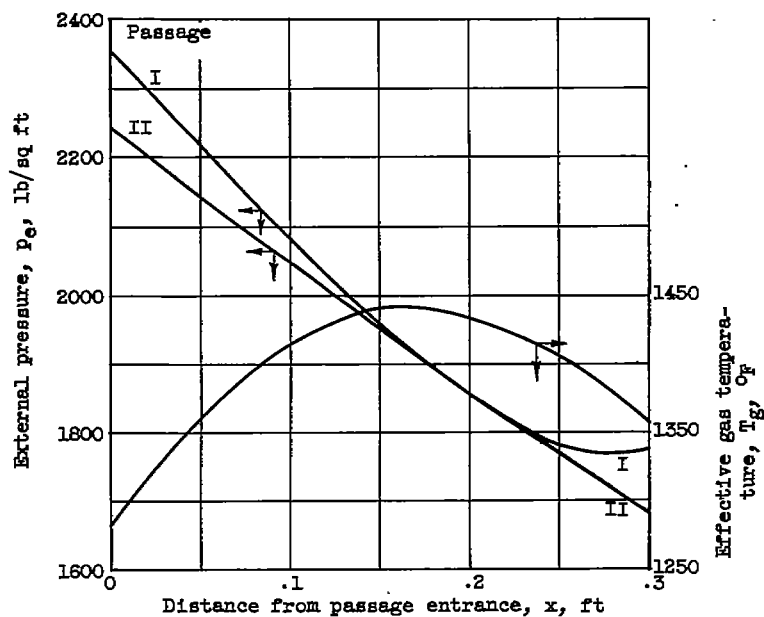
Figure 2. - Spanwise distributions of effective
gas temperature and external pressure. Angular
velocity, ω, 1205 radians per second; length, L,
0.3 foot; radius, r_r, 0.7708 foot; coolant tem-
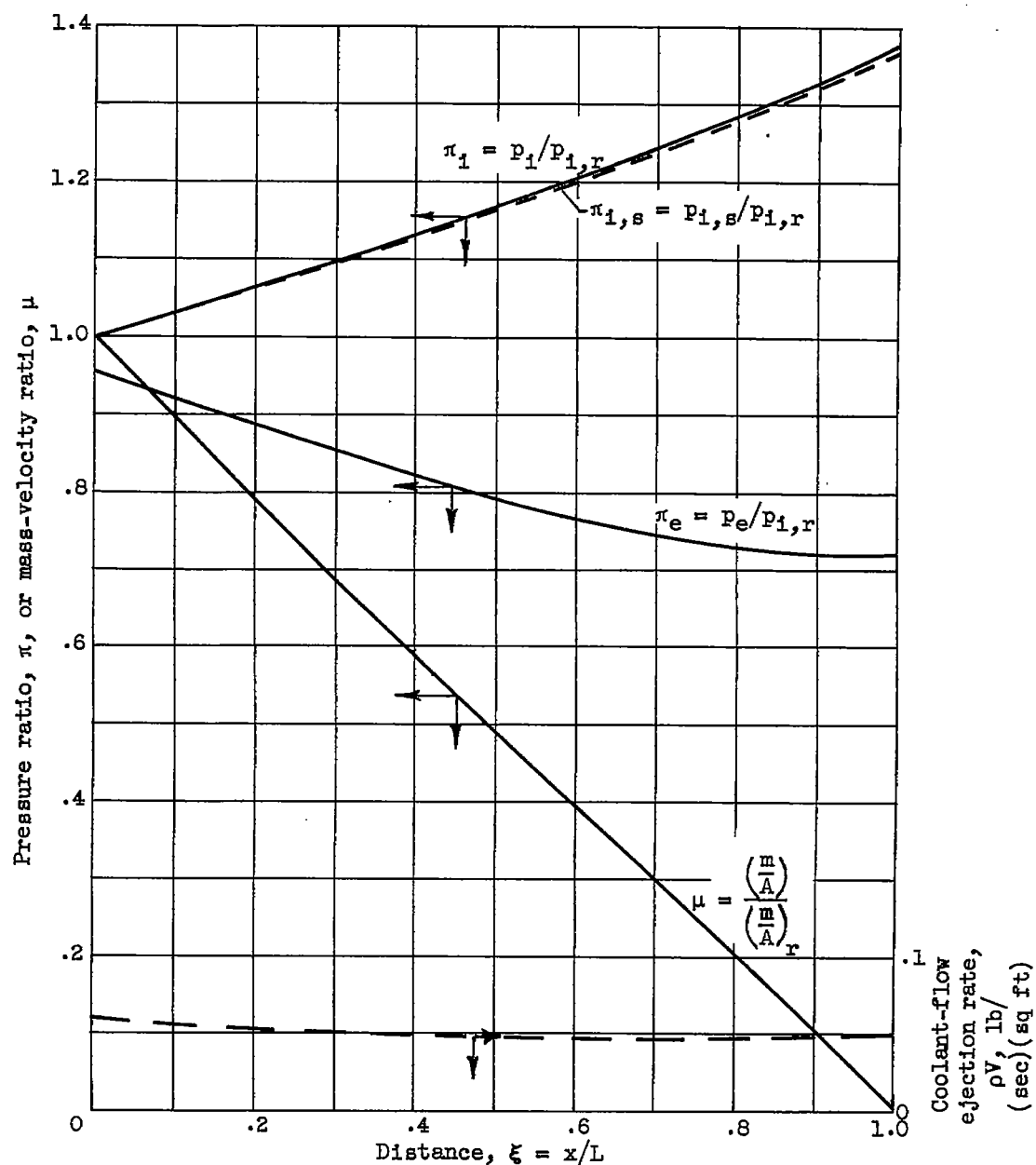perature, T, $640^\circ + 700x$ ($^\circ$R); friction factor,
f, 0.0475.

Figure 3. - Prescribed external pressure and coolant-flow ejection distributions and resulting internal pressure and coolant mass-velocity distributions for passage I.
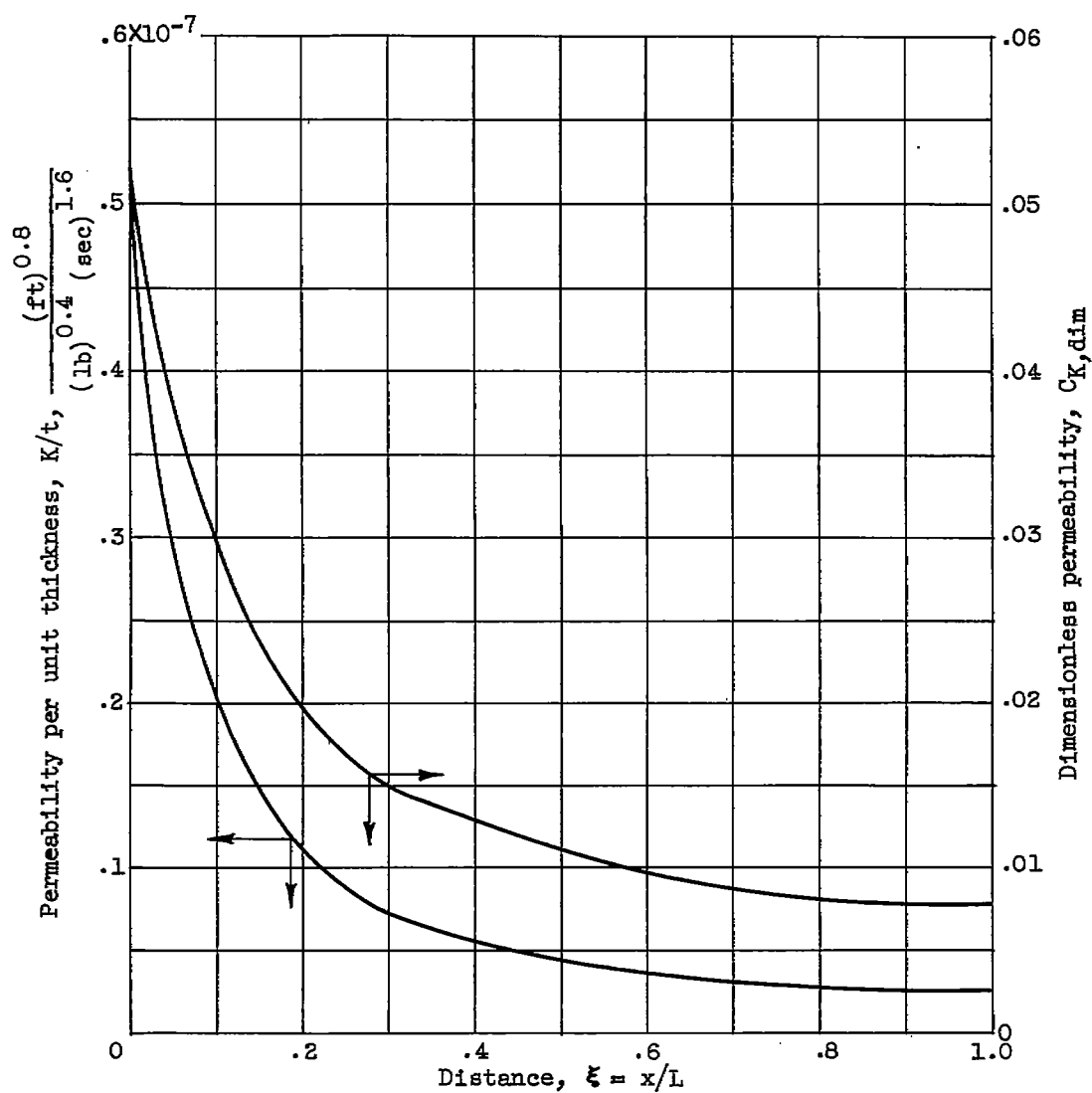
Figure 4. - Permeability distribution required to satisfy pre-
scribed coolant-flow ejection distribution for passage I.
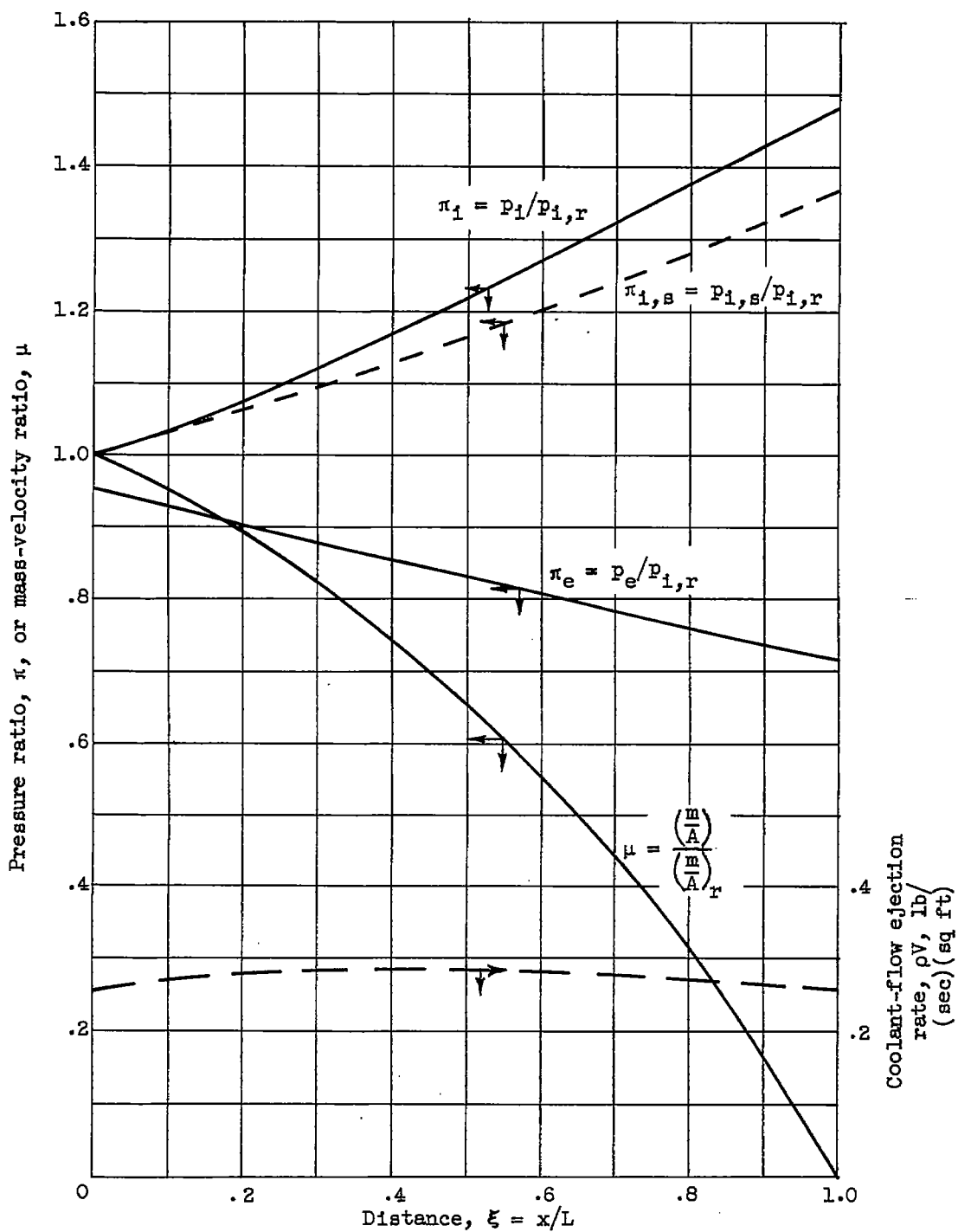
Figure 5. - Prescribed external pressure and coolant-flow ejection distributions and resulting internal pressure and mass-velocity distributions for passage II.
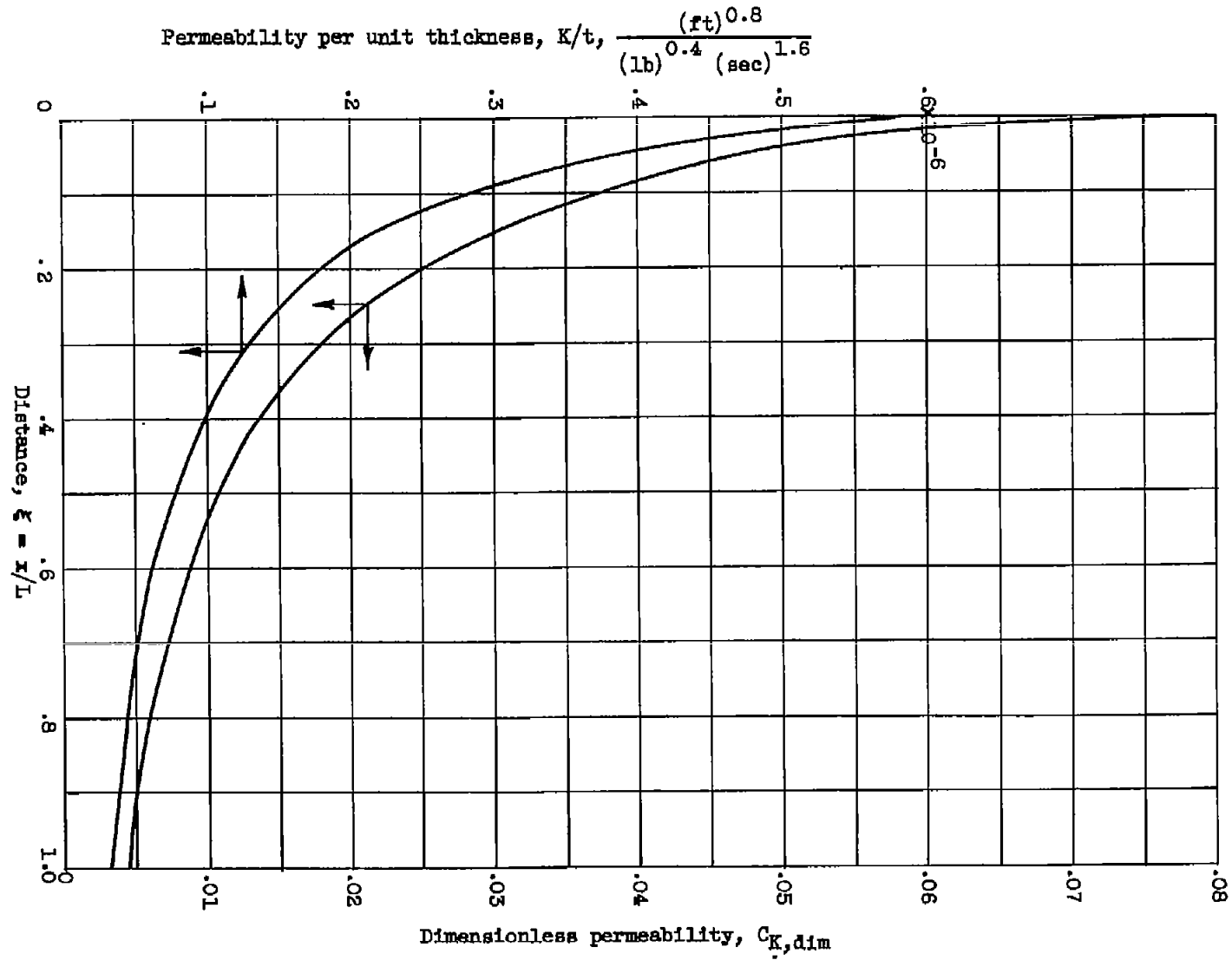
Figure 6. - Permeability distribution required to satisfy pre-scribed coolant-flow ejection distribution for passage II.

(a) External pressure.

(b) Internal pressure.
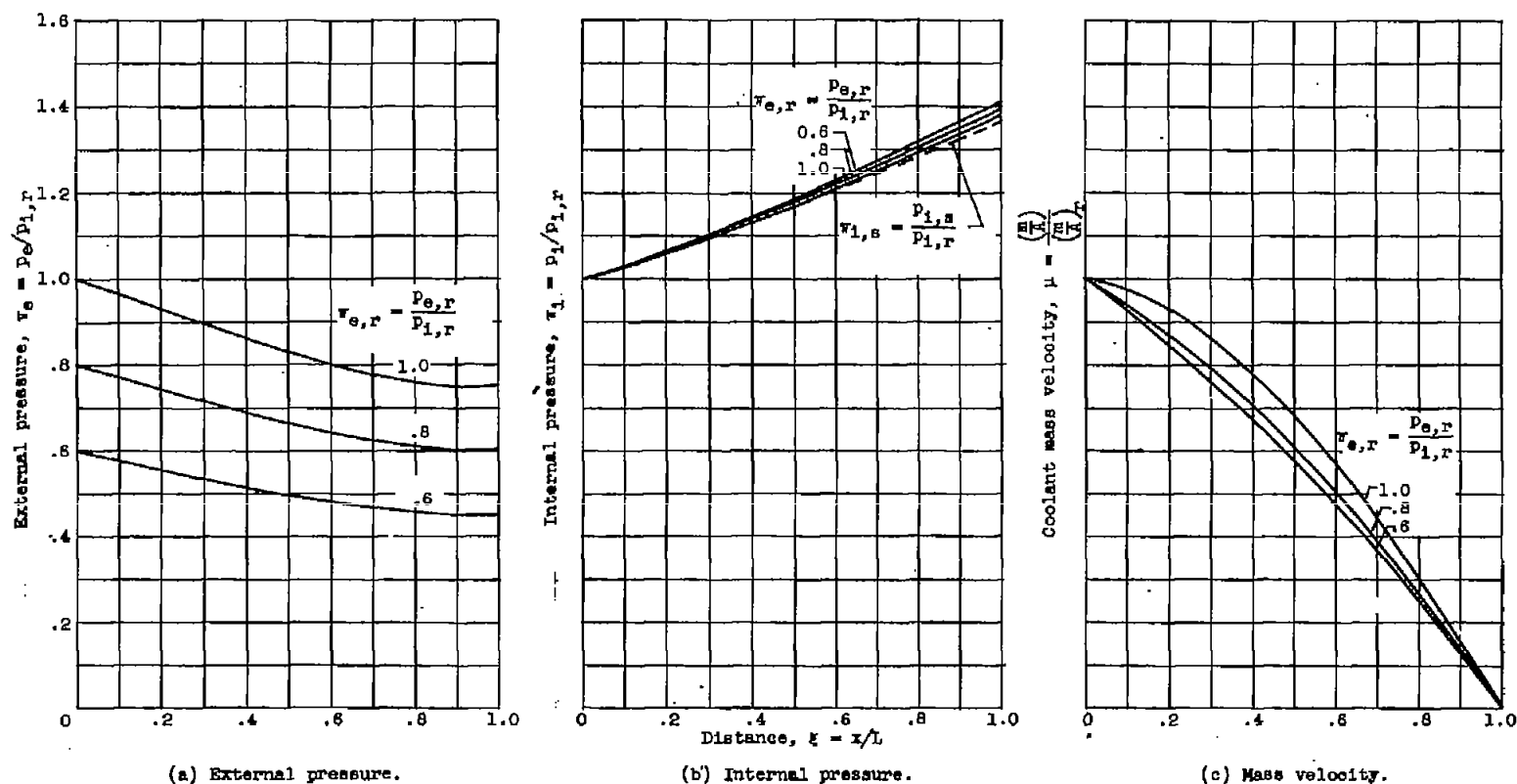
(c) Mass velocity.

Figure 7. – Effect of variation of passage inlet pressure on internal pressure and mass-velocity distributions for passage I with prescribed constant wall permeability $C_K = 10^{-5} \text{ ft}^{1/2}/(\text{sec})(\text{lb}^{1/4})$.
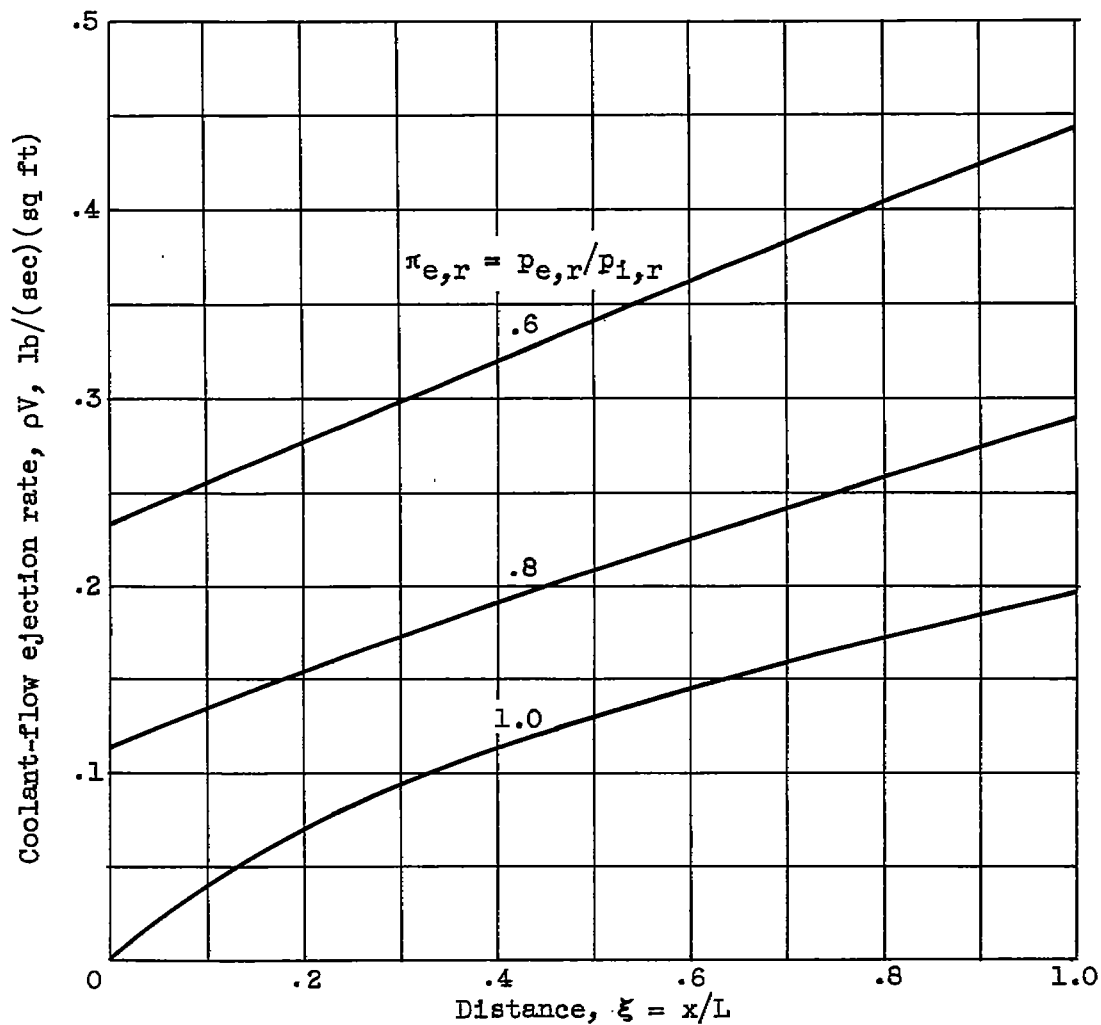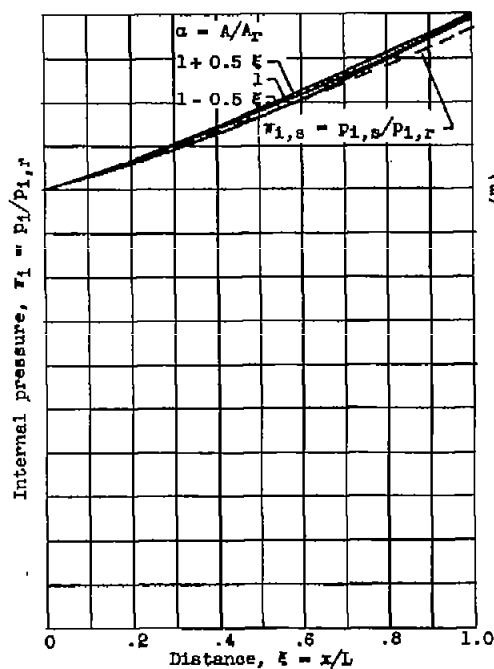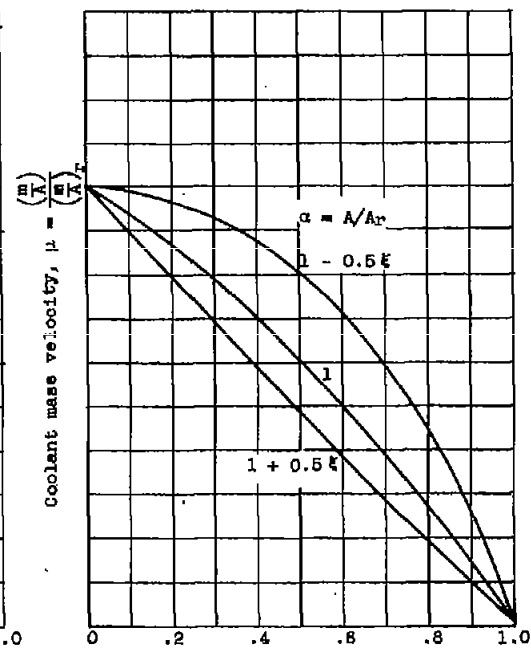
Figure 8. - Coolant-flow ejection distributions for passage I
for various inlet pressures and prescribed permeability
$C_K = 10^{-5}$ $ft^{1/2}/(sec)(lb^{1/4})$.
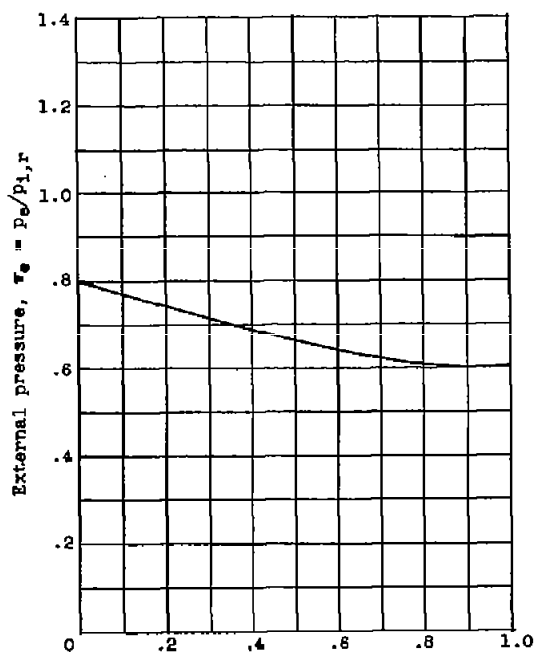
(a) External pressure.

(b) Internal pressure.

(c) Mass velocity.

Figure 9. - Effect of passage area variation on internal pressure and mass-velocity distributions for prescribed external pressure distribution and wall permeability $C_K = 10^{-5}$ ft$^{1/2}$/(sec)(lb$^{1/4}$). External pressure ratio, $\pi_{e,r} = p_{e,r}/p_{1,r} = 0.8$.
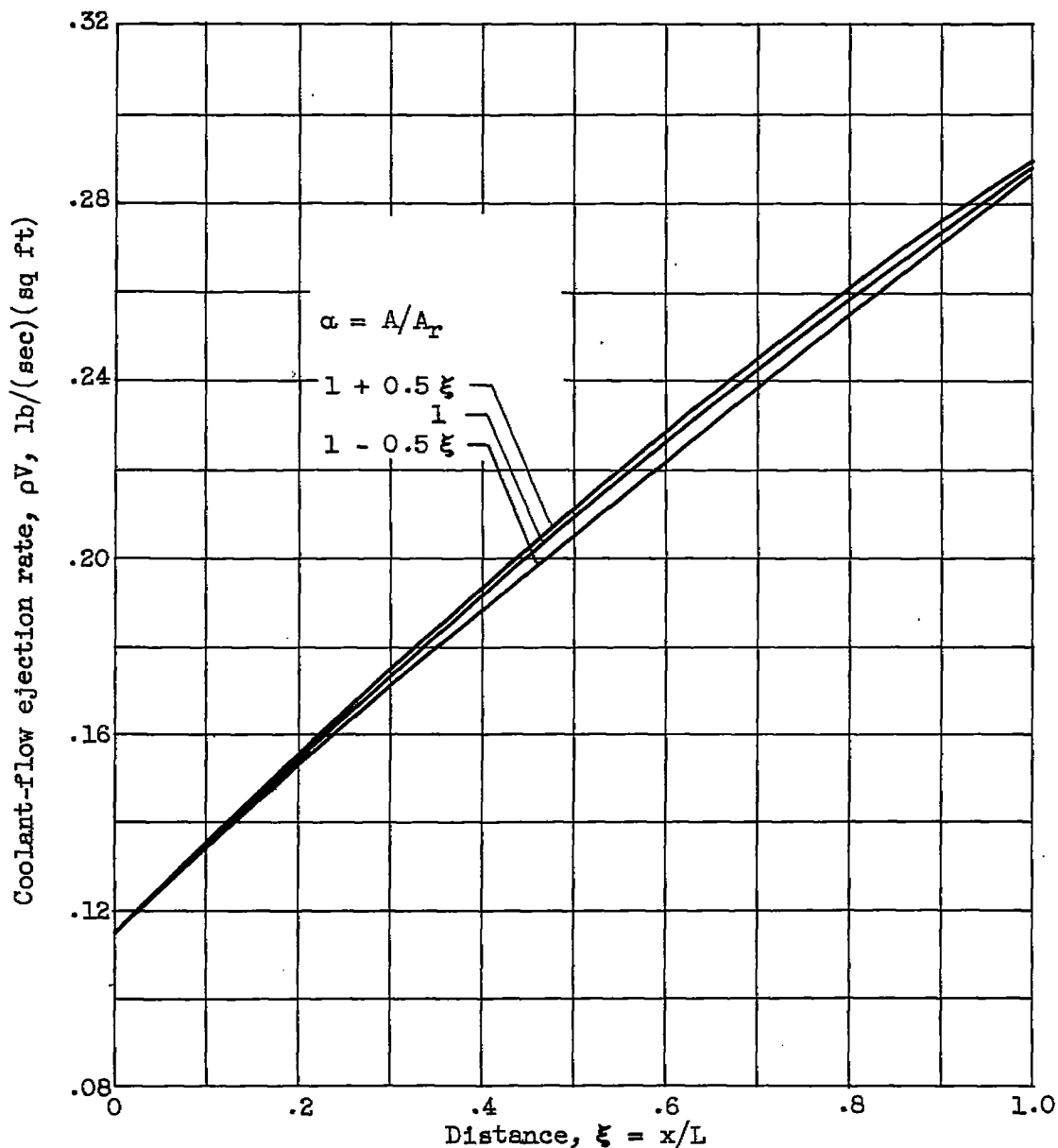
3529

Figure 10. - Coolant-flow ejection distributions for passage
with prescribed area variations, external pressure distribu-
tion, and wall permeability $C_K = 10^{-5} \, ft^{1/2}/(sec)(lb^{1/4})$.
External pressure ratio, $\pi_{e,r} = p_{e,r}/p_{1,r} = 0.8$.